Observation of Insulating Nanoislands in Ferromagnetic GaMnAs

D. M. Wang,[1] Y. H. Ren,[1,*] P. W. Jacobs,[1] S. Fahy,[2] X. Liu,[3] J. K. Furdyna,[3] V. F. Sapega,[4] and R. Merlin[1]

[1]*Department of Physics, University of Michigan, Ann Arbor, Michigan 48109-1040, USA*
[2]*Department of Physics and Tyndall National Institute, University College, Cork, Ireland*
[3]*Department of Physics, University of Notre Dame, Notre Dame, Indiana 46556, USA*
[4]*Ioffe Physico-Technical Institute, Russian Academy of Sciences, 19402 St. Petersburg, Russia*

(Received 5 January 2009; revised manuscript received 4 May 2009; published 22 June 2009)

Resonant Raman data on ferromagnetic GaMnAs reveal the existence of a new kind of defect: insulating nanoislands consisting of substitutional Mn_{Ga} acceptors surrounded by interstitial Mn_I donors. As indicated by the observation of a sharp $1S_{3/2} \rightarrow 2S_{3/2}$ Raman transition at ~ 703 cm^{-1}, the acceptor-bound holes inside the islands are isolated from the metallic surroundings. Instead, Mn-bound excitons do couple to the ferromagnetic environment, as shown by the presence of associated Raman magnon side bands. This leads to an estimate of 5–10 nm for the nanoisland radius. The islands disappear after annealing due to the removal of the Mn_I ions.

DOI: 10.1103/PhysRevLett.102.256401 PACS numbers: 71.55.−i, 75.30.Hx, 75.50.Pp, 78.30.−j

The III-Mn-V diluted magnetic semiconductor (DMS) and, in particular, GaMnAs have attracted much attention recently due to their potential applications in spintronics [1]. It is now widely accepted that the ferromagnetism in these systems arises from the hole-mediated interaction between local magnetic moments. While the majority of the Mn ions in GaMnAs exists in the form of substitutional Mn_{Ga} acceptors, a small amount also occurs as interstitial Mn_I donors. In addition to reducing the hole density, the interstitials form antiferromagnetic Mn_{Ga}-Mn_I pairs and Mn_{Ga}-Mn_I-Mn_{Ga} complexes, which reduce the number of magnetically active Mn_{Ga} ions [2,3]. A recent hot-electron photoluminescence (PL) study indicates that the holes from Mn_{Ga} form a detached impurity band for a wide range of manganese concentrations [4]. The Mn_I ions can be removed by low-temperature annealing [2,3,5].

In this Letter, we report on a resonant Raman scattering (RRS) study of GaMnAs. Consistent with recent theoretical analyses [2] as well as with the hot-PL results [4], which show evidence of the coexistence of paramagnetic (PM) and ferromagnetic (FM) regions below the Curie temperature, T_C, and infrared absorption work [6], which suggests the existence of Mn acceptors isolated from the FM environment, our results conclusively show the occurrence of a new type of defect: paramagnetic nanoislands containing magnetically-inactive Mn_{Ga} acceptors surrounded by Mn_I donors. The RRS technique has been used successfully to probe the $1S_{3/2}$ levels of Mn acceptors in insulating GaAs [7]. Our study focuses on the $1S_{3/2} \rightarrow 2S_{3/2}$ transition of isolated neutral Mn_{Ga} acceptors in DMS GaMnAs, which reveals itself as a Raman line at ~ 703 cm^{-1}. In addition, we identified several Raman sidebands as due to the interaction between magnons from the FM environment and Mn_{Ga}-bound excitons. These observations indicate that the distance between the Mn_{Ga} acceptor and the FM surroundings is $\sim$5–10 nm. We find that the hole-bound transitions disappear after the sample is annealed, and we interpret this as due to the outdiffusion of Mn_I ions [2].

We studied several FM GaMnAs films and a lightly-doped PM GaAs:Mn sample. The FM samples were grown on semi-insulating (001) GaAs substrates by low-temperature molecular-beam epitaxy (MBE). Two as-grown FM films are 300-nm thick with nominal Mn concentrations 1.4% and 2.6%, and the same Curie temperature of 44 K. The third as-grown FM film is 120-nm thick with 9% Mn and $T_C = 60$ K. A small portion of this sample was annealed for one hour in a nitrogen gas atmosphere at 270 °C. The PM sample, grown on (111) GaAs, has a concentration of 0.04% [7]. Samples were placed inside a liquid-helium flow magnetic cryostat for low temperature measurements. We used a cw Ti:sapphire laser whose wavelength λ_L could be tuned from 750 nm to 835 nm. RRS spectra were obtained with a Dilor XY system. The laser power density on the samples was ~ 8 mW/cm^2. The experiments in a magnetic field were carried out in a near-backscattering Faraday geometry with fields oriented along $\hat{z}$, the direction perpendicular to the films' surface. The Raman geometry is described using standard notation: $z(\sigma^+, \sigma^-)\bar{z}$ denotes the backscattering configuration where the incident and scattered beams are represented, respectively, by $z(\sigma^+ \text{ and } \sigma^-)\bar{z}$. Here σ^+ and σ^- stand for right and left circular polarizations, whereas z and $\bar{z}$ indicate the directions of the corresponding wave vectors.

Figure 1(a) shows RRS spectra excited at different laser wavelengths. The feature indicated by the dashed line, which appears on the high-energy side of the PL peak, is ascribed to the $1S_{3/2} \rightarrow 2S_{3/2}$ Mn acceptor transition (we note that, due to exchange coupling between the $j = 3/2$ hole and the $S = 5/2$ Mn^{2+} core, the acceptor ground state is actually a $F = 1$ multiplet [7,8]). Our assignment is supported by the facts that this peak is only observed in samples containing Mn and that its position, 703 cm^{-1}

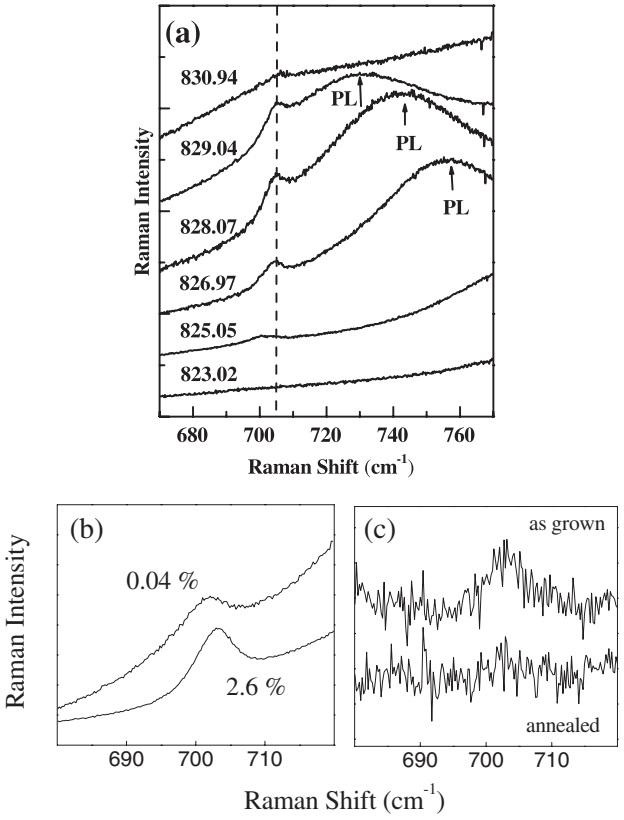

FIG. 1. (a) Data for the 1.4% Mn sample. The dashed line indicates the position of the $1S_{3/2} \rightarrow 2S_{3/2}$ acceptor transition. Numbers on the left indicate the laser wavelength, λ_L, in nm. The broad peak, PL, is due to $e - A^0$ photoluminescence. (b) Data at two, PM (0.04%) and FM (2.6%), Mn concentrations obtained with $\lambda_L = 826.5$ nm. (c) Comparison between the as-grown and the annealed 9% Mn sample after a linear background subtraction ($\lambda_L = 827.3$ nm).

(87.8 meV), agrees extremely well with the measured difference between the $1S_{3/2}$ and $2S_{3/2}$ binding energies of Mn-bound holes in GaAs [8]. Furthermore, the 703 cm^{-1} line appears only in a narrow range of *scattered* photon energies, centered at ~1.41 eV, which is very close to that of the dominant $e - A^0$ PL in GaAs:Mn arising from the recombination of electrons with Mn-bound holes [9]. These observations are consistent with a double-resonant Raman process involving excitons bound to Mn-acceptors, denoted by A^0X [7], for which the cross section can be written approximately as

$$d\sigma \propto [(E_I - E_{A^0X})^2 + \gamma^2]^{-1} \times [(E_S - E_{A^0X} + \Delta_{1S} - \Delta_{2S})^2 + \gamma^2]^{-1}.$$

Here E_I (E_S) is the incident (scattered) photon energy, E_{A^0X} and $\hbar\gamma^{-1}$ are the energy and the lifetime of the exciton, and $\Delta_{1S}(\Delta_{2S})$ is the binding energy of the $1S_{3/2}$ ($2S_{3/2}$) acceptor state. In the Raman process, the exciton created by the incident photon interacts with the bound hole, originally in the $1S_{3/2}$ state, and promotes it to the $2S_{3/2}$ level before it recombines [10]. The scattering is strongly enhanced due to both the incident and scattered resonances and, thus, it is extremely sensitive for investigating the spectrum of the impurities.

A comparison between RRS spectra of the PM and the 2.6% FM samples is shown in Fig. 1(b). Both samples exhibit relatively sharp peaks with very similar energy, linewidth ($\sim 6\ \text{cm}^{-1}$) and resonant behavior. These results strongly suggest that the feature observed in the FM sample is due to isolated acceptors, as opposed to transitions involving the $1S_{3/2}$ and $2S_{3/2}$ impurity bands [4,11,12], which should be significantly broader than those seen for the low concentration PM specimen. We believe that the presence of neutral Mn acceptors is closely related to the existence of Mn_I in the FM samples. The interstitial ions, acting as double donors, can interact with neighboring Mn_Ga ions to form Mn complexes [2,3], in the neighborhood of which, the density of free holes is reduced facilitating the existence of solitary Mn_Ga acceptors. On the other hand, the Mn_I ions can be partly removed by annealing, which causes their outdiffusion to the surface [2,3]. The effect of low-temperature annealing on the $1S_{3/2} \rightarrow 2S_{3/2}$ transition of the 9% sample is shown in Fig. 1(c). Clearly, the Raman peak disappears after annealing. This can be explained by the increase in the hole density, which opens the initially isolated Mn_Ga ions to become interactive with the FM environment. Previous measurements have shown that annealing at 250 °C for 30 minutes can increase the hole concentration by ~10%–30% and lead to an enhancement of T_C by a factor of ~1.7 [13]. Also, isolated Mn ions located outside the ferromagnetic environment have been reported to exist in the DMS InMnSb [14].

Results in an applied magnetic field, of magnitude B, reveal a strong dependence of the scattering on the polarization of the *incident* light; see Fig. 2(a). As shown in Fig. 2(b) at 2.6 K, the $1S_{3/2} \rightarrow 2S_{3/2}$ intensity increases (decreases) with increasing field if the exciting light is σ^- (σ^+) polarized. Referring to the simplified, single-particle RRS process depicted in Fig. 2(c), such a behavior can be accounted for by the Zeeman splitting of the ground $F = 1$ multiplet, for which the gyromagnetic factor is $g \sim 2.75$ [7,8], and thermal population effects. At sufficiently low temperatures, the bound holes reside for the most part in the lowest-lying state, $m_F = -1$, involving mostly $m_j = 1/2, 3/2$ states from the GaAs valence band [15]. To minimize the Coulomb repulsion between the two holes in A^0X, the Raman process is dominated by transitions associated with states that have the same magnetic quantum number. These excitations are allowed mainly in one of the two circular polarizations because of the predominance of positive values of m_j. Conversely, when the thermal energy is much larger than the Zeeman splitting, the m_F populations become comparable and, as illustrated by the 7 K data in Fig. 2(b), the difference in peak heights becomes negligible. These considerations also explain why

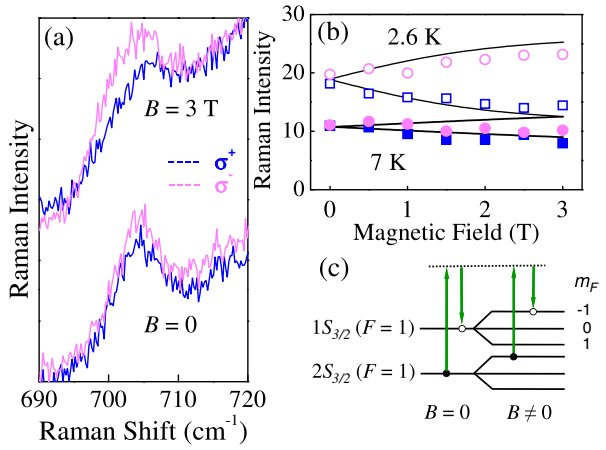

FIG. 2 (color online). (a) RRS of GaMnAs (1.4% Mn) at 2.6 K showing the dependence of the acceptor scattering on the incident photon polarization; $\lambda_L = 826.5$ nm. (b) Magnetic field dependence of the Raman intensity, in arbitrary units. Filled and open circles (squares) indicate $\sigma^-(\sigma^+-)$ polarized incident light at, respectively, 7 K and 2.6 K. The curves are from theoretical expressions described in the text. (c) Diagram showing the RRS process at zero field and in an applied magnetic field. The dashed line indicates states in the vicinity of the bottom of the GaAs conduction band. The dominant *single-particle* transitions are indicated by arrows.

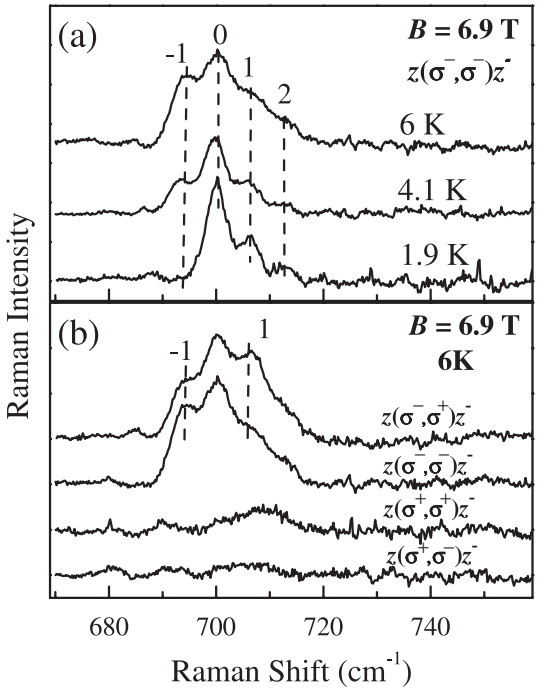

FIG. 3. RRS spectra of the sample with 2.6% Mn showing (a) the temperature dependence and (b) the scattering selection rules. The PL signal has been subtracted. Peak labeled 0 is the $1S_{3/2} \rightarrow 2S_{3/2}$ hole transition whereas -1, 1, and 2 are magnon sidebands.

the scattering does not depend on the incident light polarization at $B = 0$; see Fig. 2(a). The theoretical curves in Fig. 2(b) were obtained using the optical selection rules for zinc blende semiconductors and the acceptor wave functions listed in [15].

Figure 3 shows the temperature dependence and selection rules of the acceptor transition in the 2.6% sample at $B = 6.9$ T. At large fields, the Raman feature splits into several peaks. In addition to the central band, labeled "0", there are three sidebands marked "-1", "1" and "2" (these sidebands were not seen in the PM sample and are not resolved in the spectra of Fig. 2(a) at $B = 3$ T). The separation between neighboring peaks is nearly the same, ~ 6.6 cm^{-1}. The data of Fig. 4 shows that the splitting is proportional to the field and, thus, that it can be described by the Zeeman coupling energy $\Delta E_Z = g\mu_B B$. The experiments give $g = 2.1 \pm 0.3$, a value that agrees well with $g = 2.02$ for $3d$ Mn electrons, but differs significantly from that of Mn-bound holes with $g \sim 2.75$ [7,15]. Figure 3(a) shows that, as the temperature increases, the sidebands 1 and 2 become broader and seemingly weaker while -1 becomes stronger. Figure 3(b) shows spectra measured at different geometries at 6 K. Consistent with the results of Fig. 2, the scattering is negligible for σ^+-polarized excitation. From the figure, one sees that the -1 and 1 sidebands are strongest when the scattered light is, respectively, left (σ^-) and right (σ^+) circularly polarized. We emphasize that, unlike the FM films, no sidebands were observed in the PM sample using the same experimental conditions. From the Mn concentration in the PM sample, we estimate that the average number of Mn ions within a sphere of radius ~ 10 nm, equal to that of the acceptor-bound exciton [7], is ~ 14. Therefore, we conclude that the satellite lines appearing in the FM sample are not due to the spin-flip of a neighboring Mn ion (otherwise, these lines should also appear in the PM sample). The presence of sidebands in the FM but not in the PM sample strongly points to a connection with magnons and, accordingly, we assign the peak "-1" to the $1S_{3/2} \rightarrow 2S_{3/2}$ transition with one magnon emitted, and peaks "1" and "2" to $1S_{3/2} \rightarrow 2S_{3/2}$ excitation followed by the absorption of one and two magnons, respectively. These assignments are consistent with the temperature-dependent results and the properties of GaMnAs magnons [16]. First, we note that the measured g is consistent with our interpretation because the magnon g factor is nearly the same as that of Mn $3d$ electrons [16]. Second, the fact that the intensity of peak -1 is significantly smaller at 1.9 K supports our assignment since magnons are thermally excited and, thus, fewer magnons can be emitted at low temperatures. Finally, the observed dominance of one of the two circular polarizations in the scattering with magnon emission (sideband -1) and absorption (sideband 1) is also consistent with our interpretation since the angular momentum of the scattered photon must compensate for the change in the total spin of the magnetic system.

The occurrence of magnon sidebands indicates that some of the states involved in the RRS process interact with the FM environment. For an isolated acceptor, the

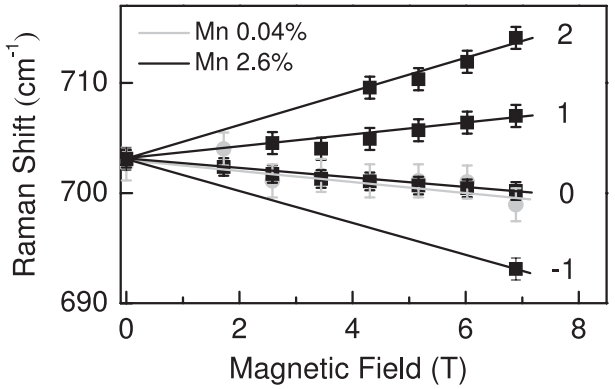

FIG. 4. Magnetic field dependence of the spectral position of the Raman features. Results are shown for the PM and the 2.6% Mn FM sample. The geometry is $z(\sigma^-, \sigma^-)\bar{z}$.

Bohr radius of the $1S_{3/2}$ and $2S_{3/2}$ states are, respectively, ~1 nm and ~5 nm [7]. Since the linewidths of the $1S_{3/2} \rightarrow 2S_{3/2}$ transition in the FM and PM samples are the same within experimental uncertainty, as shown in Fig. 1(b), it is apparent that there is little interaction between the $1S_{3/2}$ and $2S_{3/2}$ levels of the Mn_{Ga} acceptors in the islands and the FM surroundings. Therefore, the sidebands can only be the result of interactions between the FM magnons and the intermediate resonant state in the Raman process, i.e., Mn_{Ga}-bound excitons. It follows that the radius of the PM islands must be somewhere between the Bohr radius of the $2S_{3/2}$ holes (5 nm) and that of the Mn_{Ga} bound excitons (10 nm) [7]. We note that inhomogeneous structures of sizes similar to those of the nanoislands have been observed in GaMnAs using cross-sectional scanning tunneling microscopy [17].

An idealized picture of the PM nanoislands is shown in Fig. 5. The islands are insulating regions with a small concentration of holes immersed in the ferromagnetic host containing a much larger hole concentration. Their existence reflects indirectly the presence of Mn_I ions which, in itself, results from fluctuations favored by the nonequilibrium nature of low-temperature MBE [18]. The Mn_{Ga} concentration inside the islands is lower than that in the film, while the Mn_I concentration is much higher. Acting as donors, the Mn_I ions significantly reduce the density of holes inside the island where the remaining neutral Mn_{Ga} acceptors cannot interact with each other or with the ferromagnetic metallic surroundings [19]. The PM regions disappear after annealing, which removes Mn_I ions from the islands to the surface, as indicated by the disappearance of the acceptor transition in the annealed sample in Fig. 1(c).

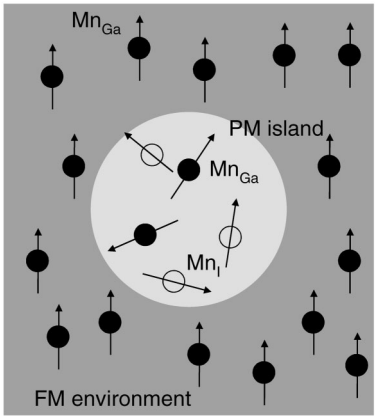

FIG. 5. Schematic diagram of a PM nanoisland. Interstitial (substitutional) ions are indicated by open (closed) circles. The island radius is ~5–10 nm. The Mn_{Ga} spins are oriented randomly inside the island, but along the same direction outside.

In summary, the $1S_{3/2} \rightarrow 2S_{3/2}$ transition of holes bound to neutral Mn acceptors and associated magnon sidebands were observed in FM GaMnAs using RRS. The results show that insulating nanoislands of 5–10 nm radius exist in as-grown samples, but disappear after low-temperature annealing due to the removal of interstitial Mn_I ions.

*Present address: Department of Physics and Astronomy, Hunter College of the City University of New York, 695 Park Avenue, NY, NY 10021, USA.

[1] H. Ohno, Science **281**, 951 (1998); K. S. Burch, D. D. Awschalom, and D. N. Basov, J. Magn. Magn. Mater. **320**, 3207 (2008).
[2] K. W. Edmonds *et al.*, Phys. Rev. Lett. **92**, 037201 (2004).
[3] K. M. Yu *et al.*, Phys. Rev. B **65**, 201303 (2002).
[4] V. F. Sapega, M. Moreno, M. Ramsteiner, L. Däweritz, and K. H. Ploog, Phys. Rev. Lett. **94**, 137401 (2005).
[5] B. S. Sørensen, P. E. Lindelof, J. Sadowski, R. Mathieu, and P. Svedlindh, Appl. Phys. Lett. **82**, 2287 (2003).
[6] Y. Nagai and K. Nagasaka, Infrared Phys. Technol. **48**, 1 (2006).
[7] V. F. Sapega, T. Ruf, and M. Cardona, Phys. Status Solidi B **226**, 339 (2001).
[8] M. Linnarsson *et al.*, Phys. Rev. B **55**, 6938 (1997).
[9] L. Montelius, S. Nilsson, and L. Samuelson, Phys. Rev. B **40**, 5598 (1989).
[10] Such resonant processes are referred to as selective-excitation PL. See, e.g., J. Wagner and M. Ramsteiner, Appl. Phys. Lett. **49**, 1369 (1986), and references therein.
[11] E. J. Singley *et al.*, Phys. Rev. B **68**, 165204 (2003).
[12] Y. J. Zhao, W. T. Geng, K. T. Park, and A. J. Freeman, Phys. Rev. B **64**, 035207 (2001).
[13] W. Limmer *et al.*, Phys. Rev. B **71**, 205213 (2005).
[14] M. Csontos *et al.*, Phys. Rev. Lett. **95**, 227203 (2005).
[15] J. Schneider, U. Kaufmann, W. Wilkening, M. Baeumler, and F. Köhl, Phys. Rev. Lett. **59**, 240 (1987).
[16] D. M. Wang *et al.*, Phys. Rev. B **75**, 233308 (2007); Y. Hashimoto, S. Kobayashi, and H. Munekata, Phys. Rev. Lett. **100**, 067202 (2008); C. Bihler, W. Schoch, W. Limmer, S. T. B. Goennenwein, and M. S. Brandt, Phys. Rev. B **79**, 045205 (2009).
[17] G. Mahieu *et al.*, Appl. Phys. Lett. **82**, 712 (2003).
[18] S. C. Erwin and A. G. Petukhov, Phys. Rev. Lett. **89**, 227201 (2002)
[19] F. Máca and J. Mašek, Phys. Rev. B **65**, 235209 (2002).